Contents lists available at ScienceDirect

EBioMedicine

EBioMedicine
Published by THE LANCET

Optogenetic augmentation of the hypercholinergic endophenotype in DYT1 knock-in mice induced erratic hyperactive movements but not dystonia

Franziska Richter *, Anne Bauer, Stefanie Perl, Anja Schulz, Angelika Richter *

Institute of Pharmacology, Pharmacy and Toxicology, Department of Veterinary Medicine, Leipzig University, An den Tierkliniken 15, 04103 Leipzig, Germany

ARTICLE INFO

ABSTRACT

Background: The most prevalent inherited form of generalized dystonia is caused by a mutation in torsinA (DYT1, ΔGAG) with incomplete penetrance. Rodent models with mutated torsinA do not develop dystonic symptoms, but previous ex vivo studies indicated abnormal excitation of cholinergic interneurons (ChI) and increased striatal acetylcholine.
Methods: We used in vivo optogenetics to exacerbate this endophenotype in order to determine its capacity to trigger dystonic symptoms in freely behaving mice. $Tor1a^{+/\Delta gag}$ DYT1 mice and wildtype littermates expressing channelrhodopsin2 under the Chat promotor were implanted bilaterally with optical LED cannulae and stimulated with blue light pulses of varied durations.
Findings: Six months old DYT1 KI mice but not wildtype controls responded with hyperactivity to blue light specifically at 25 ms pulse duration, 10 Hz frequency. Neuronal activity (c-Fos) in cholinergic interneurons was increased immediately after light stimulation and persisted only in DYT1 KI over 15 min. Substance P was increased specifically in striosome compartments in naïve DYT1 KI mice compared to wildtype. Under optogenetic stimulation substance P increased in wildtype to match levels in Dyt1 KI, and acetylcholinesterase was elevated in the striatum of stimulated DYT1 KI. No signs of dystonic movements were observed under stimulation of up to one hour in both genotypes and age groups, and the sensorimotor deficit previously observed in 6 months old DYT1 KI mice persisted under stimulation.
Interpretation: Overall this supports an endophenotype of dysregulated cholinergic activity in DYT1 dystonia, but depolarizing cholinergic interneurons was not sufficient to induce overt dystonia in DYT1 KI mice.

1. Introduction

Early-onset generalized torsion dystonia is caused by a GAG deletion in TOR1A (DYT1), which encodes for the chaperone like protein torsinA. Only 30% of the mutation carriers develop overt dystonia and the mechanisms for clinical penetrance are not known [1–3]. DYT1 knock-in (KI) mice (Tor1a$^{+/\Delta gag}$) [4] do not develop a dystonic phenotype but show sensorimotor deficits [5] probably related to cerebellothalamocortical tract changes also evident in human non-manifesting gene carriers [6]. Another consistent endophenotype across varied rodent DYT1 models is the paradoxical excitation of ChI to normally inhibitory dopamine D2 receptor activation [7]. This may be reflected in deficits in D2 receptor binding evident in manifesting and non-manifesting DYT1 mutation carriers [8,9]. Increased extracellular level of acetylcholine in DYT1 KI mice was shown to elicit this paradoxical D2 receptor response via interaction with muscarinic acetylcholine receptors [10]. Blocking these receptors ex vivo normalized D2 receptor response in striatal slices [10], while acetylcholine receptor M1 antagonists lead to normalization of synaptic plasticity [11] and rescued motor deficit in another line of DYT1 KI mice [12]. In patients, anticholinergics are effective in some cases, but the few available treatment options are insufficient or unattractive due to severe side effects [13].

High expression of Tor1a in striatal ChI could explain the preferential vulnerability of these neurons to the mutation [14,15]. ChI represent only 1–3% of striatal neurons, but they are highly branched [16,17] and critically regulate striatal signaling [18]. In DYT1 KI mice, ChI are only slightly larger and increased in number in the dorsolateral striatum [19], thus dysregulation of striatal cholinergic transmission is not associated with major structural neuroplastic changes. DYT1 KI mice also responded with increased dopamine release to nicotine [20]. Physiologically, enhanced dopamine release via nicotinic receptors provides a

---

Research in context

Evidence before this study

DYT1 dystonia is a highly debilitating and incurable movement disorder with sustained muscle contractions leading to abnormal twisting postures. Animal models are important to investigate the pathophysiology. Brain slices of rodent models carrying the DYT1 mutation were used to measure neuronal activity in the striatum. Hereby the cholinergic neurons were found to increase activity in response to dopamine, which normally reduces acetylcholine release via the D2 receptor. This finding was supported by increased extracellular acetylcholine levels in the striatum of mutated mice. However, these rodent models only show slight behavioral impairments and no dystonia. It is thus unclear whether these changes in cholinergic interneurons are related to the development of dystonic symptoms in patients.

Added value of this study

We stimulated cholinergic interneurons in vivo in a DYT1 mouse model to further increase acetylcholine levels in the striatum in a freely behaving awake animal. We established specific optogenetic stimulation parameters to increase activity of these neurons, measured by c-Fos expression. We showed that DYT1 mutated but not control mice responded with transient hyperactivity and erratic movement patterns, which did not develop into dystonic symptoms. Cholinergic interneurons in the DYT1 mutated mouse remained activated 15 min after stimulation across the entire striatum, where neurons in the control animals had already returned to baseline activity. Substance P, which is released by GABAergic neurons projecting out of the striatum, was increased in DYT1 mutant mice and after stimulation. Furthermore, acetylcholinesterase, which hydrolyzes acetylcholine and substance P, was elevated specifically in stimulated DYT1 mutated mice.

Implications of all the available evidence

Our results provide the first direct in vivo evidence that in DYT1 dystonia the function of cholinergic interneurons is altered,

negative feedback for ChI activity via D2 receptors onto ChI [21]. The lack of this feedback in DYT1 KI mice may result in an enhanced and sustained hypercholinergic tone which could influence the proper selection of movement concepts by the basal ganglia. The interaction of striatal acetylcholine and dopamine is crucial for the control of voluntary movements and an imbalance seems to play an important role in the pathophysiology of movement disorders [22].

However, the lack of an overt dystonic phenotype in this model requires further alterations to tip the balance towards penetrance. Interestingly, increase of gene dose beyond what is present in patients by conditional expression of homozygous mutations [23] or complete deletion of Tor1a from specific neurons including ChI [24] was sufficient to induce dystonia. If the hypercholinergic tone is indeed instrumental for development of overt dystonia, further exogenous stimulation of cholinergic activity may result in dystonic symptoms in heterozygous mice. Given the complex heterogeneity of the striatum, such as the distribution of acetylcholine receptor subtypes, striatal microinjections of compounds are less suitable to understand the role of a specific type of neuron in the dysfunctional striatal circuitry [25–27]. Therefore, we used in vivo optogenetics for depolarization of striatal ChI in DYT1 KI mice to test the hypothesis that a hypercholinergic tone is important for the manifestation of dystonia.

2. Methods

2.1. Animals

Animal care was in accordance with the German Animal Welfare Agency (TVV31/14, T46/16) and the European guidelines (Directive 2010/63/EU). Three or 6-month-old heterozygous DYT1 (ΔGAG) knock-in mice (DYT1 KI) (total 6 months n = 19, 3 months n = 10) and their wildtype littermates (total 6 months n = 19, 3 months n = 11) expressing channelrhodopsin-2 (ChR2) in cholinergic interneurons (ChI) were used (C57Bl/6J background). Mice were created by crossing the ChAT-IRES-Cre knock-in, which express Cre recombinase in ChI without disrupting endogenous Chat, with Ai27(RCL-hChR2(H134R)/ tdT)-D mice which express an improved ChR2/tdTomato fusion protein following exposure to Cre recombinase (Jackson Laboratory, ME, USA) [28]. Resulting homozygous offspring was crossed with DYT1 KI [4] to create heterozygous DYT1 KI/ChR2 mice and wildtype/ChR2 littermates (Fig. 1a). Genotypes were assessed by polymerase chain reaction (PCR) amplification analysis of DNA extracted from ear tissue. PCR was carried out with PuReTaq Ready-To-Go Beads (GE Healthcare) as described previously [5]. Mice were bred and housed in the institute's facility on a 12 h light/12 h dark cycle in makrolon cages (Type III, not ventilated and open to environment) at 24 °C ± 2 °C with relative humidity of about 60%. Food (Altromin standard diet) and water were available ad libitum and material for nest building was provided. Mice were single-housed starting three days prior to stereotactic surgery. All behavioral testing was carried out in the dark phase between 1 and 5 pm at low light in a dedicated experimental room. Mice were habituated for 1 h to the room prior to testing. The number of mice used in each experiment was calculated in a priori power analysis (GPower 3.1) and is provided together with the results in the text and figure legends.

2.2. Stereotactic surgery

Stereotactic surgery was performed as described previously [29,30]. Mice (male; 20–22 weeks of age, n = 13 DYT1 KI/ChR2, n = 15 wildtype/ChR2; 10 weeks of age, n = 11 DYT1 KI/ChR2, n = 10 wildtype/ChR2) were deeply anesthetized with 4.5% isoflurane (CP-Pharma, Burgdorf, Germany) and maintained at 1.6–2.0% isoflurane at a flow rate of 160–200 ml/min with 21% O_2 (Univentor 1200 Anaesthesia Unit, Univentor, Malta) inside a stereotaxic frame (Stoelting, Wood Dale, Il, USA). Ophthalmic ointment was applied for eye protection and 0.1% bupivacaine (Jenapharm, Jena, Germany) injected subcutaneously at the surgery site for peri- and postoperative analgesia. To prevent hypothermia mice were placed on isothermal pads (Braintree Scientific, MA, USA) and body temperature was recorded continuously with a rectal probe (ThermoWorks, UT, USA). A scalp incision was made midline and two holes were drilled into the skull for bilateral implantation of ultra high-power LED fiber cannulas for optogenetics (core diameter 200 μm, outer diameter 225 μm, length 2.5 mm, numerical aperture 0.66, Prizmatix, Israel) into the dorsolateral striatum according to Paxinos and Franklin's the Mouse Brain in Stereotaxic Coordinates [31] (distance to bregma anterioposterior +0.8 mm, mediolateral ± 1.9 mm and dorsoventral 2.6 mm). Three additional holes were drilled for stainless steel holding screws. Then the fibers were implanted and fixed with dental cement (Paladur, Heraeus Kulzer, Germany) to the holding screws and the skull. The skin was closed with absorbable sutures and mice were observed in their homecages until food and water intake commenced, usually in <15 min. Correct fiber placement was ascertained post mortem on coronal brain sections of all experimental animals.

2.3. Optical stimulation and behavioral analyses

After one-week recovery from stereotactic surgery, mice were habituated to the connection between implanted cannulas and the fiber
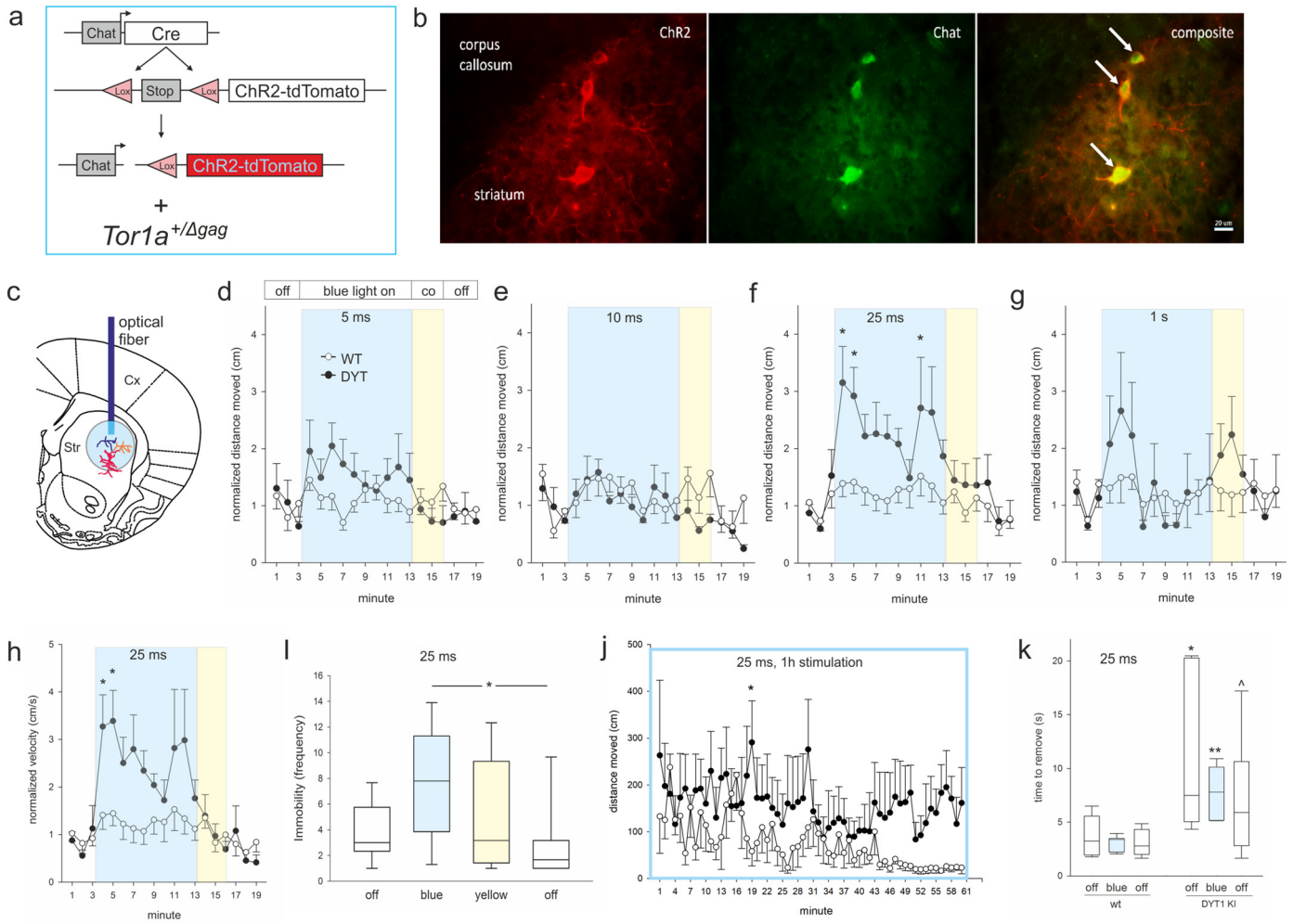
Fig. 1. (a) genetics of mouse lines used, (b) ChR2-dtTomato (ChR2, red) is expressed in ChI (Chat, green), arrows point at three striatal neurons, scale bar is 20 µm. (c) Localization of the optical fiber cannula in the dorsolateral striatum (Str). (d-g) Distance moved or (h) velocity normalized to respective baseline (mean of min 1–3) for 6 months old wildtype/ChR2 (WT, open circles) and DYT1 KI/ChR2 (DYT, closed circles) at 10 Hz and different pulse durations (5 ms and 25 ms, WT n = 11, DYT n = 8; 10 ms, WT n = 7, DYT n = 6; 1 s, WT n = 8, DYT n = 6), *p < 0.05 compared to off periods (Holm-Sidak), means ± SEM, (i) Immobility frequency at 25 ms, median, 10th, 25th, 75th and 90th percentiles, *p < 0.05 (Holm-Sidak), (j) distance moved during 60 min stimulation at 25 ms 10 Hz, WT n = 4, DYT n = 4, *p < 0.05 compared to wildtype (Holm-Sidak), (k) time to remove the adhesive sticker, median, 10th, 25th, 75th and 90th percentiles, WT n = 8, DYT n = 6, ^,*,**p < 0.1, 0.05, 0.01 versus corresponding wildtype (rank sum test).

patch cords inside their homecages (no light stimulation). On the next day mice were again connected to the fiber patch cords and placed into an open field (45 cm × 45 cm) equipped with a camera for behavioral recordings [5]. Fiber patch cords were connected to the optogenetics LEDs (Prizmatix, Israel) controlled via pulser by the behavior tracking software (EthoVision XT10, Noldus). This allowed real time behavioral analysis in relation to the specific illumination protocol used. ChI were activated by excitation of ChR2 via a 460 nm blue led light source. As control for unspecific effects of light we used a 520 nm yellow light source (Prizmatix, Israel). The power at the tip of the cannula was adjusted to 6 mW which is adequate to excite ChR2 with our setup according to the brain tissue light transmission calculator of the Deisseroth group. The correct power was verified for each fiber cannula prior to implantation and at cessation of all experiments with an optical power meter (StarLite P/N 7Z01565, Ophir Optronics, Jerusalem, Israel) as recommended previously [32]. We tested different stimulation paradigms for comparing the effects of varying optical illumination on behavior similar to previously published protocols [18,33–36]. The following protocol was used for each mouse and each stimulation paradigm: 3 min light off, 10 min blue light on, 3 min yellow light on, 3 min light off. Following pulse durations were tested: 5 ms (WT n = 11, DYT n = 8), 10 ms (WT n = 7, DYT n = 6), 25 ms (WT n = 11, DYT n = 8)

and 1 s (WT n = 8, DYT n = 6) at stimulation frequency of 10 Hz. Mice were tested in batches and the order of the protocols with different pulse durations was varied to distribute potential effects of repeated testing. In order to prevent excessive habituation to the open field, which would have reduced ambulation drastically and would not have allowed detecting a reduction in activity, mice were not habituated to the open field prior to the experiments. However, there were no significant differences in activity between the off periods prior and post optic stimulations, supporting relatively stable behavioral activity over the observation period in the open field. Parameters quantified in an unbiased fashion by the tracking software included distance moved, velocity, immobility frequency, thigmotaxis and rotation (EthoVision XT 10, Noldus). Number and duration of grooming was quantified 2 min before and 2 min into blue light stimulation by an experimenter unaware of the genotypes. One batch of mice (WT n = 8, DYT n = 6) were stimulated with blue light at 25 ms 10 Hz, which has caused the strongest behavioral response in the open field, and tested for sensorimotor deficits in the adhesive removal test [37,38] pre, during and after stimulation (3 trials each). In this test, a round sticker (1 cm diameter) was put on the bridge of the nose and the animal was immediately returned to their home cage (littermates and environmental enrichment was removed). The latency to touch the sticker and the latency to remove the sticker
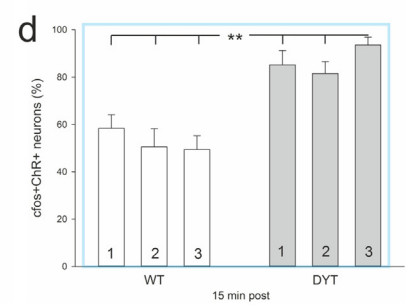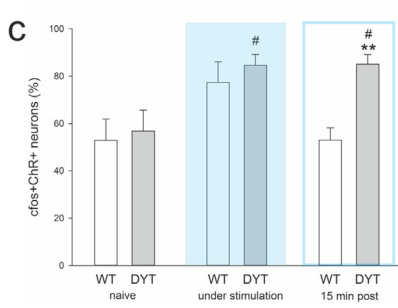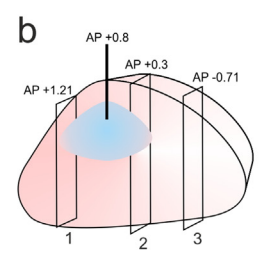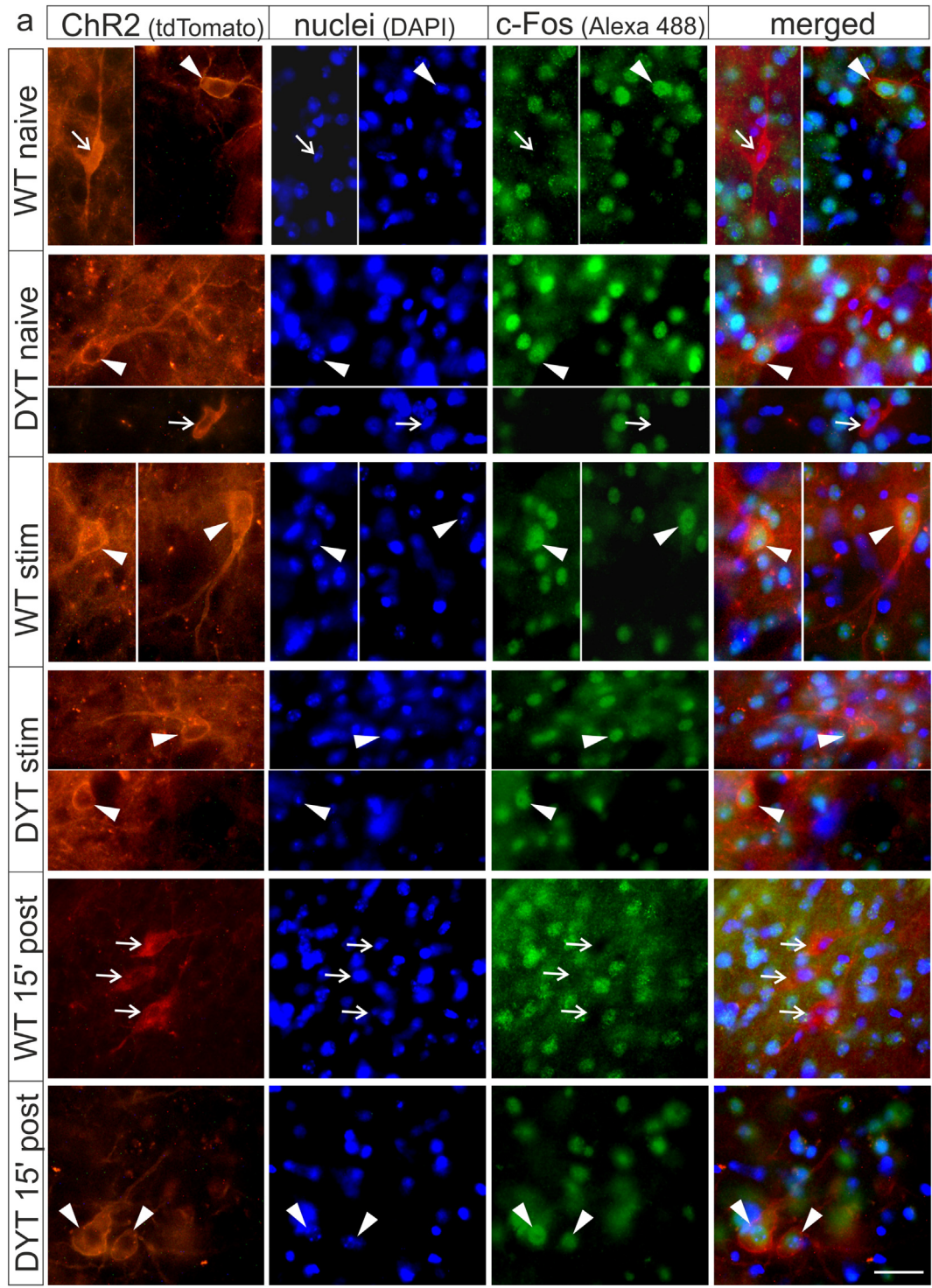
were recorded in 3 consecutive trials with a cut off time of 120 s. If mice immediately touch the sticker but have difficulty removing it, then this indicates dysfunctions of fine motor control, while a delay in touching the sticker suggests impairments of the sensory system or sensorimotor signaling pathways. First, latency to touch and to remove a sticker from the nose was measured prior to stimulation. Then mice were stimulated with blue light over 5 min and the tested under continuing stimulation. The final test followed after a 5 min period without stimulation. For immunohistochemical analysis two batches of mice were stimulated with blue light at 25 ms 10 Hz (not followed by yellow light stimulation) and sacrificed as follows: the first group over 60 min and sacrificed immediately after stimulation (WT n = 4, DYT n = 4) the second group over 10 min and sacrificed 15 min later WT (n = 6, DYT n = 5). Brains from these mice were used for quantification of neuronal activation compared to naïve controls (WT n = 4, DYT n = 6). To determine age-specific effects 3 months old mice (WT n = 10, DYT n = 11) were stimulated with 25 ms/10 Hz as follows: 3 min light off, 10 min or 30 min blue light on, 1 min light off, 3 min yellow light on, 3 min light off and sacrificed several days later 15 min after a 10 min blue light stimulation period.

2.4. Immunohistochemistry (IHC)

Tissue was processed for IHC based on previously published protocols [29,39,40]. All mice were deeply anesthetized with intraperitoneal injection of 100 mg/kg pentobarbital and perfused transcardially with 0.1 M NaCl. The brain was removed and postfixed in 4% paraformaldehyde (Pfa) dissolved in 0.1 M phosphate-buffered saline (PBS, pH 7.4) overnight by 4 °C. Brains were equilibrated for 3 days in an increasing sucrose dilution from 10 to 30% in 0.1 M PBS. Thereafter the brains were washed in 0.1 M PBS, dried, frozen on powdered dry ice and stored at −80 °C. The brains were cut in 40 μm sections on a cryostat (Hypax C 50, Zeiss, Germany) and stored at −20 °C in cryoprotectant solution (500 ml: 250 ml 0.1 M PBS, 250 ml glycerol, 0.33 g $MgCl_2$, 42.8 g sucrose). Two striatal sections of each mouse (levels AP +0.61, AP -0.23) were used for choline acetyltransferase (ChAT) IHC in order to verify expression of ChR2-dtTomato in CHI in all experimental animals. Three sections of the striatum of each mouse (levels AP +1.21, AP +0.30, AP -0.71) were used for c-Fos IHC for quantification of neuronal activity of ChR2 positive neurons. Another section of the medial striatum was used for c-Fos and substance P (SP) co-labelling. The free-floating sections were washed in 50 mM tris buffer solution (TBS, pH 7.6), followed by a blocking solution with 0.5% Triton X-100 (Tx100) and 10% normal donkey serum (NDS) in TBS or Mouse On Mouse Blocking Reagent (Vector Laboratories) for 1 h. They were incubated with primary antibody against c-Fos (Rabbit anti-c-Fos 1:200, sc-52, Santa Cruz Biotechnology, TX, USA), ChAT (Goat anti-ChAT 1:500, AB144P, Merck Millipore, Darmstadt, Germany), SP (Guinea pig anti-substance P 1:100, ab10353, Abcam, Cambridge, UK) or AChE (mouse anti-acetylcholinesterase 1:200, MAB303, Merck Millipore) in 2% NDS in TBS 24–48 h at 4 °C. Thereafter sections were washed and incubated with secondary antibodies (1:800, Donkey anti-rabbit AlexaFluor 488 or 594, Donkey anti-goat AlexaFluor 488, Donkey anti-guinea pig AlexaFluor 488, Donkey anti-mouse AlexaFluor 488, Jackson Immuno Research, Suffolk, UK) in 2% NDS and 0.5% Tx100 in TBS for 1 h. After a final wash sections were mounted on glass slides and coverslipped with VectaShield Mounting Medium with DAPI (H-1200, Vector Laboratories, CA, USA).

2.5. Image acquisition and quantification

Co-localization of ChR2-dtTomato positive and ChAT positive signal was verified using a confocal microscope (Olympus Fluoview FV 1200, Software Olympus Fluoview 4.1, Olympus, Germany). For quantification of c-Fos-, ChR2- and double-positive cells stereological analysis with the optical fractionator probe was used as published previously [39,40]. Stereo Investigator software (MBF Bioscience, VT, USA) coupled to a Zeiss Axioskop microscope with a Ludl XYZ automated motorized stage, z-axis microcator (Visitron Systems, Germany), Retiga 2000R CLR-12 colour digital camera (QImaging, Surrey, Canada) and LED light source (Cool LEDpe300, CoolLED) was used for stereological sampling. The striatum was delineated using the 10× objective and labeled neurons were counted using the 40× objective (counting frame: 100 × 100 μm, grid size: 420 × 420 μm for c-Fos, 170 × 170 μm for co-labeling ChR2 and c-Fos). Image acquisition parameters were kept constant during quantification. To measure c-Fos reactivity in single SP positive neurons of the matrix, three immunofluorescence double-labeled confocal images from the striatum were acquired at 40× under constant imaging conditions. Fluorescence intensity was measured in all SP positive neurons with the nucleus in focus using ImageJ as described previously [41]. For quantification of c-Fos and SP immunoreactivity in striosomes versus matrix, and AChE immunoreactivity in the striatum, microscopic images were acquired with the Zeiss Axioskop under constant imaging conditions and mean fluorescent intensity measured in the striosome versus matrix compartments using Image J.

2.6. Statistics

All results of behavioral testing and stereological quantification were acquired and analyzed by an investigator who was blind to group conditions. The behavioral outcomes per min were analyzed by a mixed design analysis of variance (ANOVA) (genotype × stimulation) with stimulation as repeated measure. Cell counts were quantified with ANOVA for independent variables (genotype × stimulation) for comparison across the different stimulation protocols or with ANOVA for mixed design (genotype × section) with section as repeated measure for analysis of the effect distribution across the three striatal sections. Fluorescence intensity in striosome versus matrix was analyzed by a mixed design ANOVA (genotype × region) with region as repeated measure and effects of stimulation per region via ANOVA for independent variables (genotype × stimulation). ANOVA was followed by multiple comparisons correcting post-hoc test (Holm-Sidak method). Significance was assigned at p < 0.05. Behavioral data was normalized to pre-stimulation off period in figures, but statistics were performed on raw data. Significance was assigned at p < 0.05.

3. Results

3.1. ChI stimulation elicits hyperactivity but no dystonic symptoms in DYT1 KI mice

All experimental animals expressed ChR2-dtTomato in all ChI observed in two sections of the medial striatum (Fig. 1b) and received optic stimulation in the dorsolateral striatum (Fig. 1c). At 6 months of age, DYT1 KI but not wildtype mice responded with a transient hyperactivity to ChI depolarization. Analyses of the distance moved per min in the open field uncovered a main effect of stimulation at 5 ms (F(18/306) = 2.1, p = 0.007), 10 ms (F(18/180) = 2.3, p = 0.003) and

Fig. 2. (a) Representative images of c-Fos (green) activity in ChR2-positive neurons (red) and DAPI-positive nuclei (blue) in naïve and stimulated (stim) DYT1 KI (DYT) and wildtype (WT) mice, and 15 min after stimulation (15′ post). Arrowheads point at c-Fos-positive ChR2 neurons, while open arrows point at c-Fos-negative ChR2 neurons, scale bar is 25 μm. (b) Localization of blue light stimulation and the three quantified coronal sections in the striatum. (c) percentage of ChR2-positive neurons that are c-Fos-positive in wildtype/ChR2 (WT, open bars) and DYT1 KI/ChR2 (DYT, grey bars) stimulated at 25 ms, 10 Hz with different protocols (naive, WT n = 4, DYT n = 6; 10 min light on +15 min delay before sacrifice, WT n = 6, DYT n = 5; 1 h light on, no delay before sacrifice, WT n = 4, DYT n = 4), **p < 0.01 compared to respective naïve (Holm-Sidak), #p < 0.05 compared to respective WT (Holm-Sidak), means ± SEM, (d) ChR2/c-fos positive neurons quantified for three different sections for the 10 min light on +15 min delay stimulated groups, **p < 0.01 WT versus DYT (Holm-Sidak).

25 ms (F(18/305) = 4.6, p < 0.001) but not at 1 s pulse duration (F(18/198) = 1.2, p = 0.25) (Fig. 1d-g). Posthoc tests for the respective min (1–3 light off, 4–13 blue light on, 14–16 yellow light on, 17–19 light off) revealed increased distance moved during blue light stimulation compared to light off at 25 ms pulse duration specifically in DYT1 KI/ChR2 mice (4 vs. 2 p = 0.002, 4 vs. 18 p = 0.006, 4 vs. 19 p = 0.007, 5 vs. 2 p = 0.012, 4 vs. 1 p = 0.016, 5 vs. 18 p = 0.029, 5 vs. 19 p = 0.034, 11 vs. 2 p = 0.049) but not in wildtype/ChR2 controls (Fig. 1f). At 5 or 10 ms pulse duration, there were no significant differences (Fig. 1d, e). As expected, DYT1 KI mice did not differ in their activity from wildtype at baseline [5]. Importantly, there were no effects of yellow light stimulation (posthoc p > 0.05). To further describe this transient hyperactivity phenotype we quantified velocity and immobility frequency. At 25 ms pulse duration, there was a main effect of stimulation (F(18/305) = 4.7, p < 0.001) and increase of velocity during blue light stimulation compared to light off in DYT1 KI/ChR2 (4 vs. 2 p = 0.006, 4 vs. 18 p = 0.009, 4 vs. 19 p = 0.009, 5 vs. 2 p = 0.013, 5 vs. 18 p = 0.020, 5 vs. 19 p = 0.021, 4 vs. 1 p = 0.034) but not in wildtype/ChR2 controls (Fig. 1h). The increased mobility of DYT1 KI/ChR2 under blue light was frequently interrupted by brief immobility (increased immobility frequency, blue light versus post light off p = 0.023, versus pre light off p = 0.1, Wilcoxon signed rank test; Fig. 1i), leading to an erratic hyperactive movement pattern. This phenotype was age dependent, as we did not observe genotype specific effects in 3 months old mice using comparable stimulation parameters (Fig. S1a). We hypothesized that, if this induced hyperactivity is related to development of overt dystonia, prolonged ChI stimulation may provoke dystonic symptoms. However, we did not observe signs of dystonia/dyskinesia in mice stimulated with blue light over 60 min. While wildtype/ChR2 controls habituated to the environment, DYT1 KI mice remained comparably active until end of stimulation (Fig. 1j). Similarly 3 months old DYT1 KI or wildtype mice did not show dystonic symptoms after prolonged ChI stimulation (Fig. S1b). Mice of either genotype in all experimental groups did not show changes in thigmotaxis, rotation behavior or grooming in response to stimulation (not shown). Importantly, ChI stimulation did not alter the sensorimotor phenotype we have previously described in 6 months old DYT1 KI mice (Fig. 1k, rank sum test wildtype versus DYT1 KI, p < 0.05 with or without stimulation).

3.2. ChI stimulation causes prolonged c-Fos activation in ChR2 neurons of DYT1 KI mice

Sections from the anterior, medial and posterior striatum from stimulated and naïve mice were stereologically quantified for density of c-Fos and ChR2 neurons (Fig. 2a, b). While there was no main effect of stimulation or genotype on the number of single labeled c-Fos- or ChR2-positive cells in the striatum, cell counts revealed an increase in double-positive cells in response to blue light stimulation (main effect of stimulation, (F(2/23) = 6.2, p = 0.007), Fig. 2c). Stimulation with blue light increased the number of c-Fos/ChR2 (ChI) positive neurons to 85% of all ChR2 neurons in DYT KI/ChR2 (posthoc, to naive p = 0.02) and 77% in wildtype/ChR2 (posthoc, to naive p = 0.07). In DYT1 KI/ChR2 mice this increased neuronal activity was also evident if there was a delay of 15 min between sacrifice and a 10 min stimulation (posthoc, to naive p = 0.02) while in wildtype/ChR2 neuronal activity was not different from naive (Fig. 2c). Accordingly, ANOVA revealed a main effect of genotype (F(1/23) = 6.0, p = 0.02) and posthoc a difference between c-Fos/ChR2 cell counts between genotypes in the delayed sacrifice protocol (p = 0.003). The increased percentage of c-Fos/ChR2 positive cells was present in all striatal sections even outside of direct light exposure in DYT1 KI/ChR2 mice but not in corresponding wildtype/ChR2 (main effect of genotype F(1/18) = 26.0, p < 0.001; posthoc genotype effect for each section p < 0.01, Fig. 2d). Conversely, we did not observe a prolonged c-Fos activation of ChR2 positive cells in 3 months old DYT1 KI or wildtype mice euthanized 15 min after

stimulation (Fig. S1c), which is in line with absence of hyperactivity under ChI stimulation at this age.

3.3. Increased substance P (SP) and acetylcholine esterase (AChE) expression upon ChI stimulation

Aiming to provide insights on how prolonged ChI activation in DYT1 KI mice effects downstream neurons we analyzed SP expressing striatal projection medium spiny neurons (direct pathway) for c-Fos reactivity. These neurons localize mainly to striosomes (Fig. 3a) where SP labelling was visibly enhanced and distributed in soma and dense terminals (local collaterals) as expected [42]. Specificity of staining was also confirmed by strong SP labelling of the ventral pallidum. In the matrix compartment, SP labeling distinguished sparsely distributed positive neurons (Fig. 3a). Because single neurons were difficult to distinguish in the striosomes (Fig. 3b), mean c-Fos reactivity was quantified for this compartment. In the matrix, c-Fos reactivity of SP positive neurons was measured in single slice confocal images (Fig. 3c). There was no effect of genotype (DYT1 KI versus wildtype) or stimulation (naïve versus stimulated) on mean c-Fos reactivity in the striomsomes or matrix compartments (Fig. 3d), which is in line with the observed lack of change in the total number of striatal c-Fos positive neurons described in the previous section. In the matrix, all SP positive neurons were also c-Fos positive and there was no effect of genotype or stimulation on c-Fos reactivity measured in single SP positive neurons (Fig. 3e). Striatal projection neurons release SP together with GABA. Interestingly, SP reactivity was increased in the striosome but not the matrix of naïve DYT1 KI mice compared to wildtype (region F(1/8) = 33.901, p < 0.001; genotype F(1/8) = 4.3, p = 0.071; posthoc region in wildtype p = 0.022, in DYT1 KI p < 0.001; genotype in striosome p = 0.035, in matrix p > 0.05, Fig. 4a). Upon ChI stimulation SP expression increased significantly in wildtype which was no longer different from DYT1 KI (stimulation F(1/17) = 5.6, p = 0.03; posthoc in wildtype p < 0.05).

Finally we quantified whether release of acetylcholine and SP upon ChI stimulation triggered prolonged increased expression of acetylcholinesterase (AChE). AChE efficiently catalyzes hydrolysis of acetylcholine thereby maintaining homeostasis of cholinergic synapses [43], but was also shown to hydrolyze neuropeptides, including SP [44]. AChE protein expression was increased specifically in DYT1 KI mice 15 min after cessation of stimulation compared to corresponding naïve (main effect of stimulation F(1/17) = 10.2, p = 0.005; posthoc stimulation in DYT1 KI p = 0.002, in wildtype p > 0.05, Fig. 4b), while there was not difference between naïve genotypes.

4. Discussion

Stimulations of striatal cholinergic interneurons (ChI) revealed DYT1-specific hyperactivity and erratic movement patterns in 6 months old mice, but did not induce dystonic symptoms and did not alter the sensorimotor phenotype. Our observations of hyperactivity and prolonged ChI activation after optic stimulation in DYT1 KI mice support alterations in ChI as endophenotypic trait.

Increased c-Fos activity by stimulation confirmed successful activation of ChI in vivo in our experiments. In DYT1 KI but not wildtype mice this activation persisted 15 min after stimulation. This genotype effect may be the result of different response of ChI to dopamine, which is triggered by acetylcholine via nicotinic receptors upon optic stimulation. Under physiological conditions, dopamine release pauses ChI burst activity via D2 receptors [21,45]. This mechanism would account for reset to baseline neuronal activity as observed in wildtype mice. It may also be an explanation for the absence of behavioral effects in wildtype mice. While ChI were successfully activated, the striatal circuitry did not change to the degree required for obvious behavioral alterations. This is in line with previous observations of ChI stimulation in wildtype mice [18,35]. In DYT1 KI mice, previous studies showed elevated striatal extracellular acetylcholine levels leading to a
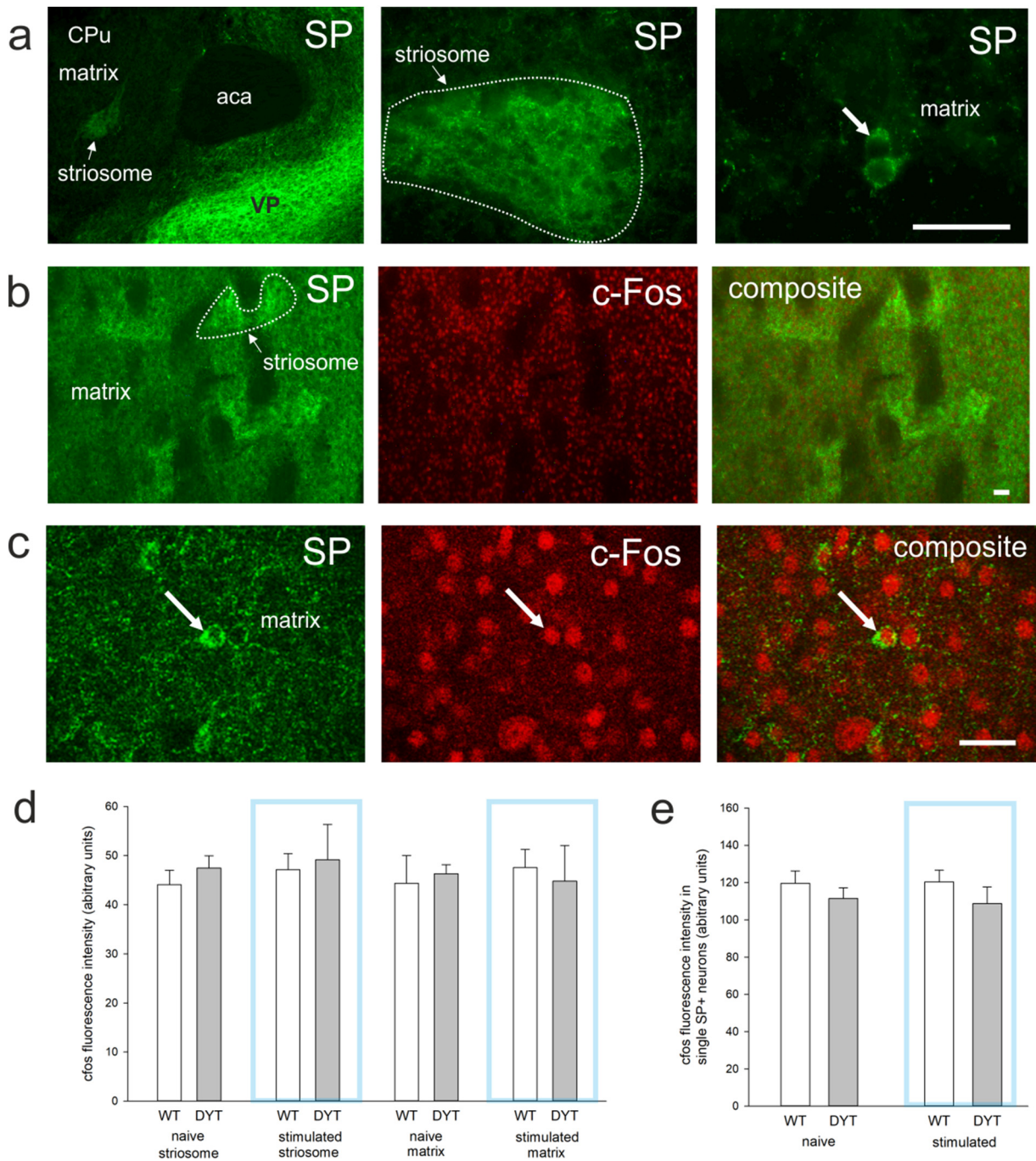
Fig. 3. (a) Substance P (SP) immunoreactivity (green) in a coronal section of the striatum (aca, anterior part of anterior commissure; VP, ventral pallidum; CPu, striatum). (b) Representative microscopic images of SP (green) and c-Fos (red) colabelling in the striatum, white outline depicts one striosome, scale bar is 50 μm. (c) Representative confocal slice with single SP and c-Fos positive neurons in the matrix, scale bar is 25 μm. (d) Bar graph with quantification of mean c-Fos immunoreactivity in striosome and matrix (naive, WT n = 4, DYT n = 6; 10 min light on +15 min delay before sacrifice, WT n = 6, DYT n = 5), mean + SEM. (e) Bar graph with quantification of c-Fos immunoreactivity in SP positive neurons in the matrix, mean + SEM.

paradoxically dopamine D2 receptor-mediated excitation of ChI via muscarinic acetylcholine receptors [10]. Therefore, in mutant mice, dopamine would not pause cholinergic activity but evoke further acetylcholine release. Furthermore, while muscarinic autoreceptor function is conserved, it would not be expected to sufficiently counteract increased acetylcholine release. This can explain the prolonged c-Fos activation of ChI beyond optogenetic stimulation in our study. Thus, at the condition of the endophenotype present in the DYT1 KI, ChI depolarization was sufficient to evoke a transient behavioral response. Localization of the fiber tip in the dorsolateral striatum was confirmed for all mice, and limitation of light transmission through brain tissue excludes

depolarization of ChI outside the striatum. Importantly, ChI are known to synchronize throughout the striatum at high activity which our data replicated by widespread ChI c-Fos activation even in parts of the striatum not exposed to light (Fig. 2d). This synchronous activation of ChI is necessary to activate nicotinic receptors on dopaminergic terminals [21]. ChR2 expression on cell processes [46] will have facilitated synchronization of widely branched ChI [47]. Follow up experiments combining optogenetics with microdialysis should give insights into torsinA related striatal neurotransmitter imbalances.

ChI are tonically active with a frequency of 5–10 Hz [48], prompting us to use 10 Hz frequency for all stimulations. Interestingly, behavioral
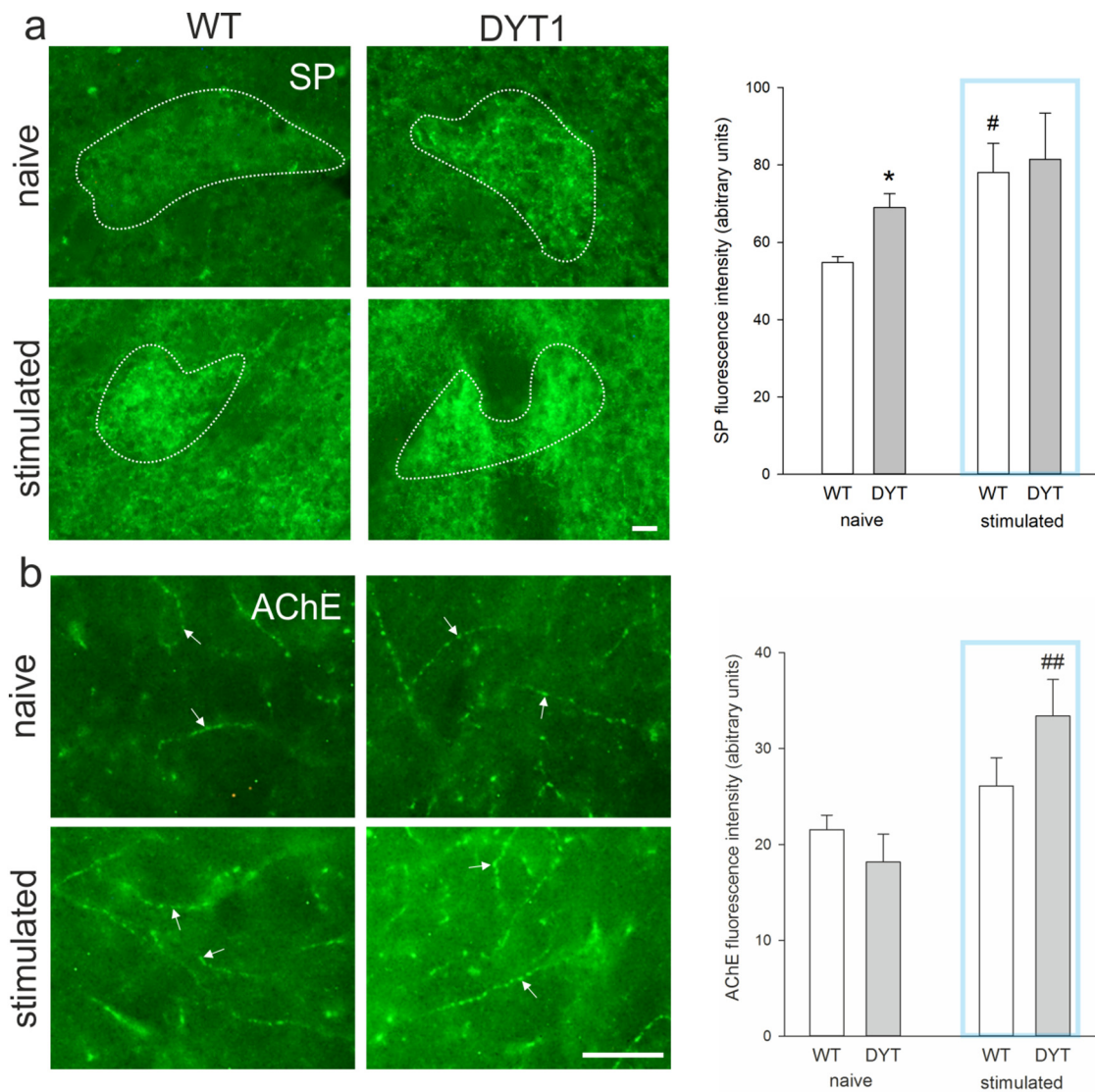
Fig. 4. Quantification of (a) substance P (SP) immunoreactivity in striosomes (white outline) and (b) acetylcholinesterase (AChE) immunoreactivity in the striatum (white arrows) of naïve and stimulated WT and DYT1 KI mice (naïve, WT n = 4, DYT n = 6; 10 min light on +15 min delay before sacrifice, WT n = 6, DYT n = 5) with representative images, scale bar is 25 μm, bar graph shows mean + SEM, *p < 0.05 WT versus DYT (Holm-Sidak), #,##p < 0.05, 0.01 WT stimulated to naïve (Holm-Sidak).

effects occurred specifically at 25 ms pulse duration in DYT1 KI. Short light pulses of 5 or 10 ms trigger single action potentials while 25 ms triggers a burst firing with an increased release of acetylcholine [21]. Durations >40 ms decrease firing rates [36]. Variability of behavioral response to different pulse durations was also observed by ChI stimulation in an animal model of levodopa induced dyskinesia [33]. Hyperactivity was transient and occurred in the first minutes after stimulation, followed by a delayed second spike. While providing more detailed insights, analysis by minute reduced statistical power due to multiple comparison corrections. If statistics is done on data collapsed over the 10 min stimulation period, hyperactivity is highly significant at 25 ms in DYT1 KI compared to pre and post off periods. The biphasic effect could be related to transient adaptive changes in the striatal circuitry to ChI depolarization, or induction of a depolarization block, a state where stimulated neurons cease to fire action potentials [36]. Silencing of neurons is a potential confounding factor of optogenetics, which may lead to conflicting behavioral alterations. However, it is more likely to occur at longer pulse durations, where we did not observe behavioral effects. The observed increase in c-fos activity of ChI at the end of the 10 min stimulation interval also supports increased activity of these neurons rather than silencing.

The hyperactive erratic activity observed in ChI stimulated DYT1 KI mice likely results from postsynaptic effects of acetylcholine and dopamine via their respective receptors onto striatal projection neurons [49]. In order to gain insights into activity of these neurons and to understand why only DYT1 KI mice responded with hyperactivity, we quantified overall c-fos and SP immunoreactivity in the striatum, as well as c-fos reactivity in SP positive neurons. SP is co-released with GABA by the subset of striatal GABAergic medium spiny neurons that project directly to the basal ganglia output nuclei. Thereby SP accumulates in striosomes where these neurons are preferentially located [50]. Increased expression of SP in striosomes of naïve DYT1 KI mice versus wildtype, and upon ChI stimulation, will have facilitated overall excitability via presynaptic NK1 receptors on glutamatergic inputs [51] and boosted dopamine release in striosome centers [50]. This is in line with the observed hyperactivity phenotype, which is a common feature of animal models with increased striatal dopamine levels [52,53]. In fact, hyperactivity in hyperdopaminergic mice is frequently associated with impaired habituation to the environment [54], similar to our observations of higher activity after prolonged stimulation (Fig. 1j). Interestingly, all SP positive neurons were also c-fos positive, with comparable signal intensity, independent of genotype, optogenetic stimulation or hyperactivity

response. Similarly, quantification of the overall number of all c-fos positive striatal neurons, mostly representing projection neurons, did not reveal differences. Therefore c-fos may not be a sensitive marker for further increase of neuronal activity in these neurons as opposed to the increase observed in ChI. Importantly, ChI express NK1 receptors and are depolarized by SP [55]. Therefore increased reactivity for SP may contribute to a hypercholinergic tone in DYT1 KI mice and upon optogenetic stimulation. Whether NK1 receptors may represent a potential therapeutic target in dystonia can be debated. NK1 receptor binding was unchanged in the phenotypic hamster model of dystonia [56]. Together with lack of dystonic symptoms in DYT1 KI mice even after prolonged ChI stimulation this argues against a crucial involvement of SP signaling in dystonia. Increase in AChE protein we observed specifically in DYT1 KI mice 15 min after cessation of stimulation supports the genotype specific increased response to ChI stimulation. AChE may have counteracted increased acetylcholine release upon stimulation, and thus dampened cumulative effects over prolonged stimulation. However, elevated postsynaptic SP release and observed behavioral responses argue against a full and immediate compensation. Interestingly, we did not observe elevated AChE protein in naïve DYT1 KI mice compared to wildtype. Unchanged protein level does not preclude increased enzymatic activity found in a transgenic DYT1 mouse model [57]. A lack of compensatory increase in AChE protein would explain why there were no genotype specific differences of low dosages of the AChE inhibitor neostigmine in DYT1 KI mice [10]. Regardless, the stimulation specific increase in AChE protein demonstrates that optic ChI stimulation triggered further alterations specifically in hypercholinergic DYT1 KI mice, which was the purpose of the approach.

Sensorimotor deficits were not altered by ChI stimulation, indicating that this phenotype is related to more complex cerebello-thalamocortical tract changes rather than localized striatal pathophysiology [5]. However, the co-occurrence of hypercholinergic and sensorimotor endophenotypes at 6 months of age but not in younger animals supports a prolonged age-dependent impact of the TorsinA mutation, which however did not result in dystonic symptoms under ChI stimulation. The complete lack of penetrance of dystonic symptoms in this model diverts from the reality in patients, where dystonic symptoms appear during or bevor early adulthood [58]. Technical limitations hampered the use of mice younger than 3 months (early adulthood) for chronic implantation of optogenetic fibers. Therefore, we cannot exclude that ChI stimulation before 3 months of age could elicit dystonic symptoms. Alternatively, it may be an early loss of ChI function that is responsible for the development of dystonia-like symptoms as shown in DYT1 models with severe degeneration of ChI in the dorsal striatum [24,59].

Altogether our data supports ChI malfunction upon TorsinA mutation, but increasing ChI activity with our approach was not sufficient for penetrance of dystonic symptoms in the DYT1 mouse model. Given the complexity of the striatal neuronal network, other interneurons may play an important role in further tipping the balance towards overt symptoms in the model and in patients with TorsinA mutation.

Supplementary data to this article can be found online at https://doi.org/10.1016/j.ebiom.2019.02.042.

References

[1] Martino D, Gajos A, Gallo V, et al. Extragenetic factors and clinical penetrance of DYT1 dystonia: an exploratory study. J Neurol 2013;260(4):1081–6.
[2] Lohmann K, Klein C. Genetics of dystonia: what's known? What's new? What's next? Mov Disord 2013;28(7):899–905.
[3] Walter M, Bonin M, Pullman RS, et al. Expression profiling in peripheral blood reveals signature for penetrance in DYT1 dystonia. Neurobiol Dis 2010;38(2):192–200.
[4] Goodchild RE, Kim CE, Dauer WT. Loss of the dystonia-associated protein torsinA selectively disrupts the neuronal nuclear envelope. Neuron 2005;48(6):923–32.
[5] Richter F, Gerstenberger J, Bauer A, Liang CC, Richter A. Sensorimotor tests unmask a phenotype in the DYT1 knock-in mouse model of dystonia. Behav Brain Res 2017;317:536–41.
[6] Ulug AM, Vo A, Argyelan M, et al. Cerebellothalamocortical pathway abnormalities in torsinA DYT1 knock-in mice. Proc Natl Acad Sci U S A 2011;108(16):6638–43.
[7] Eskow Jaunarajs KL, Bonsi P, Chesselet MF, Standaert DG, Pisani A. Striatal cholinergic dysfunction as a unifying theme in the pathophysiology of dystonia. Prog Neurobiol 2015;91-107:127–128C.
[8] Carbon M, Niethammer M, Peng S, et al. Abnormal striatal and thalamic dopamine neurotransmission: genotype-related features of dystonia. Neurology 2009;72(24):2097–103.
[9] Perlmutter JS, Mink JW. Dysfunction of dopaminergic pathways in dystonia. Adv Neurol 2004;94:163–70.
[10] Scarduzio M, Zimmerman CN, Jaunarajs KL, Wang Q, Standaert DG, McMahon LL. Strength of cholinergic tone dictates the polarity of dopamine D2 receptor modulation of striatal cholinergic interneuron excitability in DYT1 dystonia. Exp Neurol 2017;295:162–75.
[11] Maltese M, Martella G, Madeo G, et al. Anticholinergic drugs rescue synaptic plasticity in DYT1 dystonia: role of M1 muscarinic receptors. Mov Disord 2014;29(13):1655–65.
[12] Dang MT, Yokoi F, Cheetham CC, et al. An anticholinergic reverses motor control and corticostriatal LTD deficits in Dyt1 DeltaGAG knock-in mice. Behav Brain Res 2012;226(2):465–72.
[13] Jankovic J. Medical treatment of dystonia. Mov Disord 2013;28(7):1001–12.
[14] Augood SJ, Martin DM, Ozelius LJ, Breakefield XO, Penney Jr JB, Standaert DG. Distribution of the mRNAs encoding torsinA and torsinB in the normal adult human brain. Ann Neurol 1999;46(5):761–9.
[15] Sciamanna G, Hollis R, Ball C, et al. Cholinergic dysregulation produced by selective inactivation of the dystonia-associated protein torsinA. Neurobiol Dis 2012;47(3):416–27.
[16] Zhou FM, Wilson CJ, Dani JA. Cholinergic interneuron characteristics and nicotinic properties in the striatum. J Neurobiol 2002;53(4):590–605.
[17] Bonsi P, Cuomo D, Martella G, et al. Centrality of striatal cholinergic transmission in basal ganglia function. Front Neuroanat 2011;5(6).
[18] Maurice N, Liberge M, Jaouen F, et al. Striatal cholinergic interneurons control motor behavior and basal ganglia function in experimental parkinsonism. Cell Rep 2015;13(4):657–66.
[19] Song CH, Bernhard D, Bolarinwa C, Hess EJ, Smith Y, Jinnah HA. Subtle microstructural changes of the striatum in a DYT1 knock-in mouse model of dystonia. Neurobiol Dis 2013;54:362–71.
[20] Zimmerman CN, Eskow Jaunarajs KL, Meringolo M, et al. Evaluation of AZD1446 as a therapeutic in DYT1 dystonia. Frontiers in systems neuroscience, vol. 1; 2017; 43.
[21] Threlfell S, Lalic T, Platt NJ, Jennings KA, Deisseroth K, Cragg SJ. Striatal dopamine release is triggered by synchronized activity in cholinergic interneurons. Neuron 2012;75(1):58–64.
[22] Aosaki T, Miura M, Suzuki T, Nishimura K, Masuda M. Acetylcholine-dopamine balance hypothesis in the striatum: an update. Geriatr Gerontol Int 2010;10(Suppl. 1):S148–57.
[23] Liang CC, Tanabe LM, Jou S, Chi F, Dauer WT. TorsinA hypofunction causes abnormal twisting movements and sensorimotor circuit neurodegeneration. J Clin Invest 2014;124(7):3080–92.
[24] Pappas SS, Darr K, Holley SM, et al. Forebrain deletion of the dystonia protein torsinA causes dystonic-like movements and loss of striatal cholinergic neurons. Elife 2015;4:e08352.
[25] Rossi MA, Calakos N, Yin HH. Spotlight on movement disorders: what optogenetics has to offer. Mov Disord 2015;30(5):624–31.
[26] Lenz JD, Lobo MK. Optogenetic insights into striatal function and behavior. Behav Brain Res 2013;255:44–54.
[27] Hamann M, Plank J, Richter F, et al. Alterations of M1 and M4 acetylcholine receptors in the genetically dystonic (dt(sz)) hamster and moderate antidystonic efficacy of M1 and M4 anticholinergics. Neuroscience 2017;357:84–98.
[28] Madisen L, Mao T, Koch H, et al. A toolbox of Cre-dependent optogenetic transgenic mice for light-induced activation and silencing. Nat Neurosci 2012;15(5):793–802.

[29] Helmschrodt C, Hobel S, Schoniger S, et al. Polyethylenimine nanoparticle-mediated siRNA delivery to reduce alpha-synuclein expression in a model of Parkinson's disease. Molecular therapy Nucleic acids, vol. 9; 2017; 57–68.

[30] Richter F, Subramaniam SR, Magen I, et al. A molecular tweezer ameliorates motor deficits in mice overexpressing alpha-synuclein. Neurotherapeutics 2017;14(4): 1107–19.

[31] Paxinos G, Franklin K. Paxinos and Franklin's the mouse brain in stereotaxic coordinates. . 4th ed.Academic Press; 2012.

[32] Sparta DR, Stamatakis AM, Phillips JL, Hovelso N, van Zessen R, Stuber GD. Construction of implantable optical fibers for long-term optogenetic manipulation of neural circuits. Nat Protoc 2011;7(1):12–23.

[33] Bordia T, Perez XA, Heiss J, Zhang D, Quik M. Optogenetic activation of striatal cholinergic interneurons regulates L-dopa-induced dyskinesias. Neurobiol Dis 2016;91: 47–58.

[34] Nelson AB, Hammack N, Yang CF, Shah NM, Seal RP, Kreitzer AC. Striatal cholinergic interneurons drive GABA release from dopamine terminals. Neuron 2014;82(1): 63–70.

[35] Witten IB, Lin SC, Brodsky M, et al. Cholinergic interneurons control local circuit activity and cocaine conditioning. Science 2010;330(6011):1677–81.

[36] Herman AM, Huang L, Murphey DK, Garcia I, Arenkiel BR. Cell type-specific and time-dependent light exposure contribute to silencing in neurons expressing Channelrhodopsin-2. Elife 2014;3:e01481.

[37] Fleming SM, Salcedo J, Fernagut PO, et al. Early and progressive sensorimotor anomalies in mice overexpressing wild-type human alpha-synuclein. J Neurosci 2004;24 (42):9434–40.

[38] Lam HA, Wu N, Cely I, et al. Elevated tonic extracellular dopamine concentration and altered dopamine modulation of synaptic activity precede dopamine loss in the striatum of mice overexpressing human alpha-synuclein. J Neurosci Res 2011;89(7): 1091–102.

[39] Richter F, Gabby L, McDowell KA, et al. Effects of decreased dopamine transporter levels on nigrostriatal neurons and paraquat/maneb toxicity in mice. Neurobiol Aging 2017;51:54–66.

[40] Bode C, Richter F, Sprote C, et al. Altered postnatal maturation of striatal GABAergic interneurons in a phenotypic animal model of dystonia. Exp Neurol 2017;287:44–53 Pt 1.

[41] Richter F, Fleming SM, Watson M, et al. A GCase chaperone improves motor function in a mouse model of synucleinopathy. Neurotherapeutics 2014;11(4):840–56.

[42] Hutcherson L, Roberts RC. The immunocytochemical localization of substance P in the human striatum: a postmortem ultrastructural study. Synapse 2005;57(4): 191–201.

[43] Dobbertin A, Hrabovska A, Dembele K, et al. Targeting of acetylcholinesterase in neurons in vivo: a dual processing function for the proline-rich membrane anchor subunit and the attachment domain on the catalytic subunit. J Neurosci 2009;29(14): 4519–30.

[44] Chubb IW, Hodgson AJ, White GH. Acetylcholinesterase hydrolyzes substance P. Neuroscience 1980;5(12):2065–72.

[45] Goldberg JA, Reynolds JN. Spontaneous firing and evoked pauses in the tonically active cholinergic interneurons of the striatum. Neuroscience 2011;198:27–43.

[46] Zeng H, Madisen L. Mouse transgenic approaches in optogenetics. Prog Brain Res 2012;196:193–213.

[47] Contant C, Umbriaco D, Garcia S, Watkins KC, Descarries L. Ultrastructural characterization of the acetylcholine innervation in adult rat neostriatum. Neuroscience 1996; 71(4):937–47.

[48] Wilson CJ, Goldberg JA. Origin of the slow afterhyperpolarization and slow rhythmic bursting in striatal cholinergic interneurons. J Neurophysiol 2006;95(1):196–204.

[49] Quartarone A, Hallett M. Emerging concepts in the physiological basis of dystonia. Mov Disord 2013;28(7):958–67.

[50] Brimblecombe KR, Cragg SJ. Substance P weights striatal dopamine transmission differently within the Striosome-matrix Axis. J Neurosci 2015;35(24):9017–23.

[51] Blomeley CP, Kehoe LA, Bracci E. Substance P mediates excitatory interactions between striatal projection neurons. J Neurosci 2009;29(15):4953–63.

[52] Richter F, Richter A. Genetic animal models of dystonia: common features and diversities. Prog Neurobiol 2014;121:91–113.

[53] Chesselet MF, Richter F. Modelling of Parkinson's disease in mice. Lancet Neurol 2011;10(12):1108–18.

[54] Zhuang X, Oosting RS, Jones SR, et al. Hyperactivity and impaired response habituation in hyperdopaminergic mice. Proc Natl Acad Sci U S A 2001;98(4):1982–7.

[55] Aosaki T, Kawaguchi Y. Actions of substance P on rat neostriatal neurons in vitro. J Neurosci 1996;16(16):5141–53.

[56] Friedman Y, Richter A, Raymond R, Loscher W, Nobrega JN. Regional decreases in NK-3, but not NK-1 tachykinin receptor binding in dystonic hamster (dt(sz)) brains. Neuroscience 2002;112(3):639–45.

[57] Martella G, Tassone A, Sciamanna G, et al. Impairment of bidirectional synaptic plasticity in the striatum of a mouse model of DYT1 dystonia: role of endogenous acetylcholine. Brain 2009;132:2336–49 Pt 9.

[58] Ozelius LJ, Lubarr N, Bressman SB. Milestones in dystonia. Mov Disord 2011;26(6): 1106–26.

[59] Pappas SS, Li J, LeWitt TM, Kim JK, Monani UR, Dauer WT. A cell autonomous torsinA requirement for cholinergic neuron survival and motor control. Elife 2018;7.